

# TREATING OMICRON BA.4 & BA.5 VIA HERBAL ANTIOXIDANT ASAFOETIDA: A DFT STUDY OF CARBON NANOCARRIER IN DRUG DELIVERY

FATEMEH MOLLAAMIN <sup>1\*</sup>, SARA SHAHRIARI <sup>2</sup> AND MAJID MONAJJEMI <sup>3</sup>

<sup>1</sup>Department of Biomedical Engineering, Faculty of Engineering and Architecture, Kastamonu University, Kastamonu, Turkey.

<sup>2</sup>Department of Chemistry, Central Tehran Branch, Islamic Azad University, Tehran, Iran.

<sup>3</sup>Department of Chemical Engineering, Central Tehran Branch, Islamic Azad University, Tehran, Iran.

## ABSTRACT

Currently, the results of researches have exhibited that Omicron sub-lineages BA.4 and BA.5, evaluated to BA.1 and BA.2, deserted neutralization from sera of triple vaccinated particulars to a bigger extension. Therefore, a novel wave of Omicron virus has appeared driven by BA.4 & BA.5 subvariants. Nanocarriers contain carbon atoms with functional nanostructures, which not only help the improved mechanical properties but also indicate the bioactivities for regulating cell status. In this research, asafoetida as a medicinal plant can be applied in treatment for Omicron subvariants BA.4 and BA.5 through adsorbing of its effective compound of ferulic acid on the surface of (6,6) armchair single-walled carbon nanotube as the drug delivery model due to direct electron transfer principle which has been studied by density functional theory (DFT) methods.

On the other hand, it has been accomplished the B3LYP/6-311+G (d,p) level of theory to evaluate the aptitude of SWCNT for adsorbing effective compound in asafoetida medicinal plant through nuclear magnetic resonance and thermodynamic parameters. In fact, the achieved results have represented that the feasibility of using (6,6) armchair SWCNT and ferulic acid becomes the norm in drug delivery system which has been attained by quantum calculations due to physico-chemical properties of NMR, IR and UV-VIS spectroscopy. Besides, the energy gap analysis of HOMO-LUMO has illustrated the charge distribution in the frontier molecular orbitals of ferulic acid in asafoetida drug through adsorption on the surface of (6,6) armchair carbon nanotube (CNT).

**Keywords:** Omicron subvariants BA.4 and BA.5, Asafoetida; Ferulic acid; CNT; drug delivery.

## 1. INTRODUCTION

During the COVID-19 pandemic, the new BA.2 subvariant has quickly substituted by old subvariants BA.1 and BA.1.1. The latter finding of three serious Omicron subvariants has increased in some concerns [1-7].

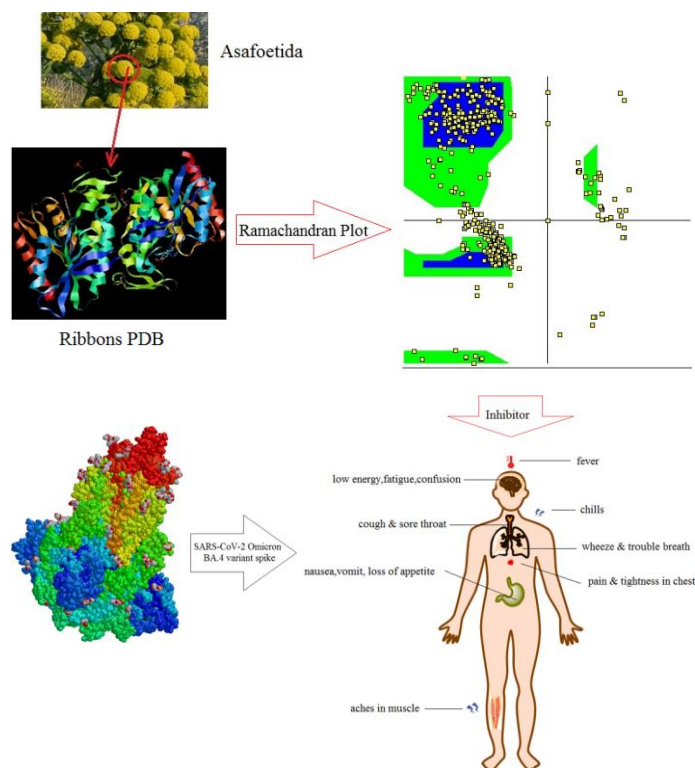
Besides, in the United States, the subvariant of BA.2.12.1 entered then was developed considerably in the northeast zone. Omicron subvariants of BA.4 and BA.5 appeared in South Africa became main variants. These new Omicron subvariants have been detected worldwide, though at low levels presently. However, their growth trajectories in the U.S. and South Africa exhibit an important transmission advantage.

The replacements in the BA.4 & BA.5 RBDs, L452R, and F486V are the most problem because of their possibility to allow immune attack. On the other hand, both these mutations are close to the angiotensin-converting enzyme 2 (ACE2) receptor surface, therefore might modify RBD-ACE2 association and the neutralizing capacity of natural and vaccine acquired immunity. While the reversion mutation Q493, which also exists in the ACE2, likely decreases the escape from respond to previous SARS-CoV-2 types. Currently, major variants of COVID-19 pandemic have been introduced as SARS-CoV-2 Omicron subvariants BA.4 and BA.5. The spike protein of BA.2.12.1 42 includes L452Q and S704L alterations plus to the recognized mutations in BA.2, while the 43 spike proteins of BA.4 and BA.5 are similar [8-11].

For decades, herbs and medicinal plants for decades have been considered as treatment viral diseases treatment. These medicinal plants could apply as strong origins for novel antiviral drugs versus rising and increasing viral diseases such as COVID-19 and different subvariants of Omicron virus. In this work, it has been studied that asafoetida might be an inhibitor of the Omicron subvariants BA.4 and BA.5 which is exhibited for the cure of sick people. The impact of asafoetida might decrease in patients having an impaired immune system. Asafoetida is a perennial herb with a little thick root, fleshy, cut and dusty leaves, fleshy stem, yellow flowers with umbrella-like groups and up to two meters height [12, 13].

The medicinal organ of this plant is a resinous gum obtained by cutting the upper parts of the root. Resin, essential oil, gum, ferulic acid and disulfide compounds are among the effective ingredients of asafoetida. The medicinal function of this plant is anti-flatulent and expectorant and it is used in the treatment of indigestion or colic related to flatulence, bronchitis, cough and nervous disorders [12]. The substantial amounts of native species of asafoetida are grown in the mountains of Afghanistan and the deserts of Iran [14].

Therefore, we have investigated the structural, electronic, physical and chemical characteristics of ferulic acid which is one the most effective compounds in asafoetida that might be applied to treat the Omicron subvariants BA.4 and BA.5 through relieving different side-affects in human body [Scheme 1].



**Scheme 1.** Herbal antioxidant of asafoetida, ribbons PDB and Ramachandran plot as the inhibitor of SARS-CoV-2 Omicron BA.4 and BA.5 variant spikes for relieving different side-affects in human body.

There is an attention to enhancing the bioavailability and duration of action for a drug to modify therapeutic consequences. Drug delivery technique is able to change a drug's pharmacokinetics and specificity by formulating it with various

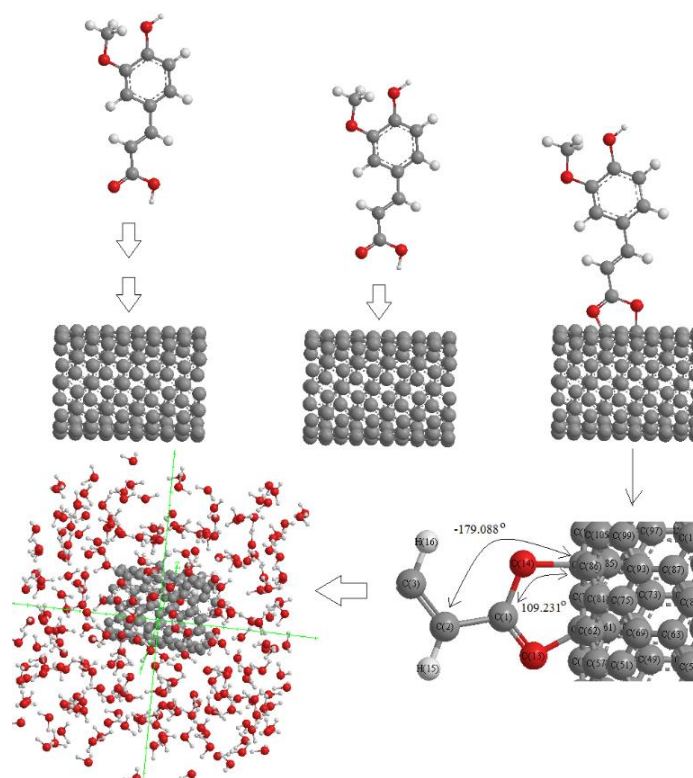
\*Corresponding author email: [smollaamin@gmail.com](mailto:smollaamin@gmail.com)

ingredients, drug carriers, and the medical equipment [15-19]. Nanomedicine in drug delivery is for achieving the improved delivery of water insoluble drugs, delivery of large macromolecule drugs to intracellular sites of action, and codelivery of two or more drugs or therapeutic agents for combination remedy [20-22].

Nanotubes with their intrinsic properties have been considered potential candidates for drug delivery carriers. The capped ends of nanotubes may be opened up by oxidation, allowing for the insertion of molecules of interest inside the nanotube. Carbon nanotubes (CNTs) can easily penetrate cells,

delivering drugs directly to the cytoplasm or nucleus. Nanotubes conform to a perpendicular position with the cell membrane during uptake, perforating and diffusing through the lipid bilayer to enter the cytoplasm. Functionalized CNTs are easily internalized by cells through passive and endocytosis-independent mechanisms [23-30].

In this research, we have ferulic acid in asafoetida adsorbed on surface of (6,6) armchair CNT in water medium for preventing the activity of Omicron subvariants BA.4 and BA.5 (Scheme2).



**Scheme2.** Mechanism of adsorption of ferulic acid on the surface of (6,6) armchair SWCNT in water medium.

The structure of ferulic acid has been studied in this article which is an effective component in the herbal antioxidant of asafoetida for adsorption on the surface of (6, 6) armchair CNT through drug delivery methodology (Scheme2). Therefore, a DFT method has been run for finding the optimized coordination of ferulic acid adsorbed on the surface of (6, 6) armchair CNT by using Gaussian 16 revision C.01 program [31].

## 2. THEORETICAL BACKGROUND, MATERIAL AND METHOD

In this article, the geometry coordination of ferulic acid in asafoetida has been optimized at the framework of DFT using the three-parameter Becke's exchange [32] and Lee-Yang-Parr's correlation non-local functional [33], usually known as B3LYP method and basis set of 6-311+G(d,p). The density functional theory (DFT) is one of the most employed approximations of Hohenberg, Kohn and Sham which allows the theoretical study of material properties [34]. Density functional theory (DFT) represents an advantageous methodology for estimating the chemical systems, and discovering its similarities and differences to other computational employed methodologies [35, 36]

Therefore, it has been illustrated the electronic structure of adsorbed (6,6) armchair CNT by ferulic acid in asafoetida medicinal plant for measuring physico-chemical properties (Scheme2).

In this work, the Onsager model has been accomplished that was developed by Frisch, Wong and Wiberg utilizes spherical cavities. Even though this implies a less accurate description of the solute-solvent interface, this approximation simplifies the evaluation of energy formatives in geometry optimizations, and frequency analysis. Moreover, Cramer and Truhlar improved this model at the

dipole level [37-41]. In fact, a cavity must have a physical sense such as Onsager model, and has a mathematical ability as often happened in other descriptions of solvent impacts [42]. On the other hand, the cavity has to keep out the solvent and including its frontiers as the biggest probability part of the solute charge distribution [43-45].

Basically, a group of quantum theoretical methods has been run for exploring some physical and chemical properties from optimized structure of ferulic acid in asafoetida medicinal plant adsorbed on the surface of (6,6) armchair CNT including charge distribution, thermodynamic calculations, nuclear magnetic resonance analysis, frontier orbitals of HOMO & LUMO analysis and UV-VIS discussion due to designing a drug delivery model y using Gaussian 16 revision C.01 program [31].

Moreover, the gauge including atomic orbitals (GIAO) has been adopted to solve the gauge problem in the calculation of nuclear magnetic shielding for ferulic acid in asafoetida adsorbed on the surface of (6,6) armchair CNT using density functional theory (DFT) calculation [46].

## 3. RESULTS AND DISCUSSION

Carbon nanotubes can easily penetrate cells, delivering drugs directly to the cytoplasm or nucleus. These compounds describe drug delivery platforms that may be functionalized with various biomolecules containing antibodies, proteins, and DNA. This permits the particular target for transferring the special tissues, organs, or cells. Drug delivery systems improve the pharmacological and therapeutic profile and efficacy of the drug and lower the occurrence of off-targets.

### 3.1. Analysis of NMR spectroscopy

Chemical shielding eigenvalues of  $\sigma_{11}$ ,  $\sigma_{22}$ ,  $\sigma_{33}$  (ppm), isotropic shielding tensor ( $\sigma_{iso}$ ), and anisotropic shielding tensor ( $\sigma_{aniso}$ ) for ferulic acid in asafetida medicinal plant adsorbed on the surface of (6,6) armchair SWCNT, respectively, have been obtained. The calculations have been accomplished based on B3LYP/6-311+G (d,p) level of theory by using Gaussian 16 revision C.01 program (Table1).

SCF GIAO magnetic shielding tensor in ppm for H, C, O atoms and exploring the active site of ferulic acid in asafetida as the natural drug for treatment the Omicron subvariants BA.4 and BA.5 has been drawn (Figure1a&b).

**Table1.** Chemical shielding of eigenvalues  $\sigma_{11}$ ,  $\sigma_{22}$ ,  $\sigma_{33}$  (ppm), isotropic shielding tensor ( $\sigma_{iso}$ ) and anisotropic shielding tensor ( $\sigma_{aniso}$ ), also atomic charge (Q) of H, C, O atoms in ferulic acid extracted from asafetida medication using SCF GIAO theoretical method.

Atom	$\sigma_{11}$	$\sigma_{22}$	$\sigma_{33}$	$\sigma_{iso}$	$\sigma_{aniso}$	Q
C1	-15.6372	161.9188	172.1630	106.1482	99.0222	0.3004
C2	44.5827	160.8814	220.0070	141.8237	117.2749	-0.0972
C3	18.7049	131.5717	212.1846	120.8204	137.0463	-0.0181
C4	78.6689	113.1457	242.8672	144.8939	146.9599	-0.0325
C5	68.8765	117.8510	231.2939	139.3404	137.9302	-0.0509
C6	83.5398	99.7001	197.7125	126.9841	106.0926	0.1129
C7	73.3400	94.6507	203.9283	123.9730	119.9329	0.1122
C8	63.7010	136.2266	218.9721	139.6332	119.0084	-0.0920
C9	55.0970	117.9162	222.1804	131.7312	135.6738	-0.0427
O10	267.8883	379.3201	404.3846	350.5310	80.7804	-0.2543
C11	170.1602	178.7827	231.0085	193.3171	56.5370	-0.0321
O12	298.6211	317.3092	326.7566	314.2290	18.7914	-0.2976
O13	-681.1946	-260.7962	442.1589	-166.6106	913.1543	-0.2909
O14	146.0424	301.2683	338.0813	261.7973	114.4259	-0.3178
H15	19.9683	25.2453	32.1288	25.7808	9.5220	0.0812
H16	19.6684	24.8934	31.4550	25.3390	9.1741	0.0793
H17	17.1551	26.7581	31.8257	25.2463	9.8691	0.0770
H18	21.8600	29.3262	29.8229	27.0030	4.2298	0.0540
H19	20.5091	28.2600	29.4811	26.0834	5.0966	0.0643
H20	24.6065	27.1074	37.9428	29.8856	12.0859	0.0706
H21	24.9868	29.2757	35.5131	29.9252	8.3819	0.0683
H22	25.0105	29.2715	35.5234	29.9351	8.3824	0.0681
H23	22.7081	29.1619	40.3955	30.7552	14.4605	0.2170
H24	22.9685	24.8511	35.9453	27.9216	12.0355	0.2208

The ferulic acid has approximately shown the fluctuation behavior (30-350 ppm) for various atoms in the active sites of these compounds through the NMR properties (Figure1a). The sharpest peak of NMR spectrum for ferulic acid has been almost observed in 30 ppm, and the weakest peaks of NMR spectrum have approximately appeared in about 100 ppm, 150 ppm, 200 ppm, 250 ppm, 300 ppm, and 350ppm, respectively (Figure1a).

The ferulic acid adsorbed on the (6,6) armchair CNT has shown the chemical shielding including  $\sigma_{11}$ ,  $\sigma_{22}$ ,  $\sigma_{33}$  and  $\sigma_{iso}$ ,  $\sigma_{aniso}$  (ppm) for various atoms of H, C, O in the active sites of the molecule through the NMR graph (Figure1b). The most fluctuations of atomic charge and chemical shielding have been observed in O10,O12, O13, O14, respectively (Table1), due to exploring the most electronegative atoms for adsorbed on the surface of (6,6) armchair CNT which represent the maximal shift in TMS B3LYP/6-311+G(d,p) (Figure1a&b).

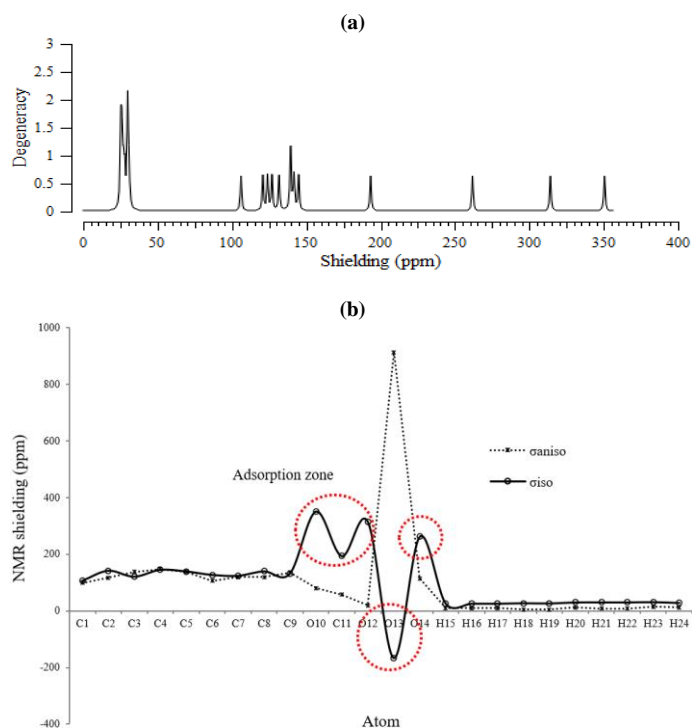


**Figure1.** a) NMR spectrum with SCF GIAO method. b) Chemical shielding of isotropic ( $\sigma_{iso}$ ) and anisotropic ( $\sigma_{aniso}$ ) calculated by level of theory B3LYP/6-311+G(d,p) for ferulic acid adsorbed on the surface of (6,6) armchair CNT.

In fact, the chemical shift tensors are achieved by the quantum chemical calculations in principal axes system to guess the isotropic chemical-shielding and anisotropic chemical-shielding [47-49].

### 3.2. Atomic Charge diffusion

The optimized atomic charge (Q) of H,C,O atoms (Table1) in a polar medium of water solution indicates the stability of ferulic acid in asafetida drug joint to the surface of (6, 6) armchair CNT as a drug delivery method for healing the Omicron subvariants BA.4 and BA.5 (Figure2). Besides, it has been exhibited the Electrostatic Potential Map (ESP) which indicates the region including attractive - repulsive force of a fixed charged at different points in space that are parallel from a molecular surface of ferulic acid (Figure2).

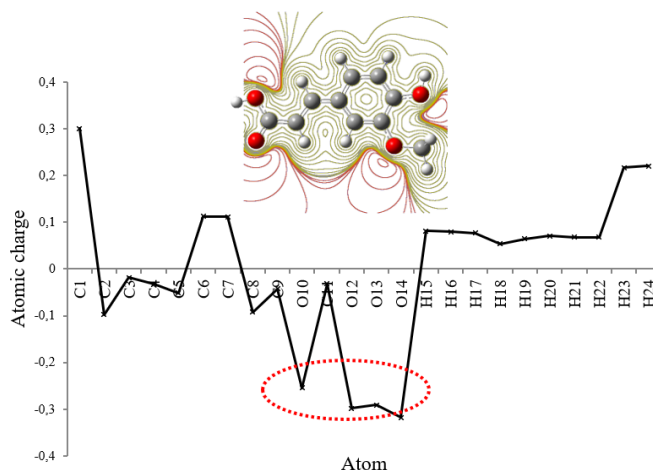


**Figure2.** The atomic charge (Q) of H, C, O atoms in the active sites of ferulic acid in asafetida medicinal plant accompanying ESP map.

It has been recommended the reason for existing stability of ferulic acid adsorbed on the surface of (6,6) armchair SWCNT which is principally bound to the position of active sites of labeled H,C,O which move the charge of electrons in this compound in polar water molecules (Figure2).

On the other hand, the electrophilic side chains of ferulic acid in asafetida medicinal plant conduct us to find the reason for the activity and the stability of this drug against the Omicron subvariants BA.4 and BA.5 in human body.

### 3.3. Analysis of Infrared spectrum

It has been resulted the infrared (IR) spectrum for ferulic acid adsorbed on the surface of (6,6) armchair CNT using B3LYP method and 6-311+G (d,p) basis set for atoms including H,C,O atoms for obtaining the more accurate equilibrium geometrical parameters, thermodynamic properties. The IR spectrum for ferulic acid in asafetida drug has been shown in the frequency range about 50 cm<sup>-1</sup>-4500 cm<sup>-1</sup> (Figure 3). It can be seen that the strongest allowed peaks with highest intensities occur about 50 cm<sup>-1</sup>, 150 cm<sup>-1</sup>, 250 cm<sup>-1</sup>, 625 cm<sup>-1</sup>, 1400 cm<sup>-1</sup>, 1450 cm<sup>-1</sup>, 1550 cm<sup>-1</sup>, 1650 cm<sup>-1</sup>, 1700 cm<sup>-1</sup>, 1750 cm<sup>-1</sup>, 1800 cm<sup>-1</sup>, 2000 cm<sup>-1</sup>, 2100 cm<sup>-1</sup>, 2150 cm<sup>-1</sup>, 2200 cm<sup>-1</sup>, and 3500 cm<sup>-1</sup>, respectively (Figure3).

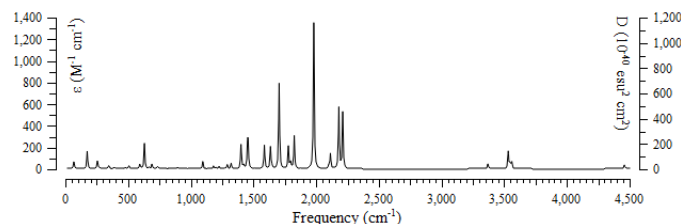


**Figure3.** The infrared spectrum of ferulic acid as the effective compound in asafetida drug adsorbed on the surface of (6,6) armchair CNT using 6-311+G(d,p) calculations.

Figure3 demonstrates the reason for existing observed various results frequencies of ferulic acid adsorbed on the surface of (6,6) armchair CNT which presents the position of active sites of labeled H, C, O atoms in asafetida medication. The calculations of the relative harmonic frequencies, IR intensities in various normal modes and thermodynamic properties of  $\Delta H$ ,  $\Delta G$ ,  $\Delta S$  for ferulic acid adsorbed on the surface of (6,6) armchair CNT using B3LYP/6-311+G(d,p) method have been reported in Table2.

**Table 2.** The results of calculated functions of harmonic frequencies (cm<sup>-1</sup>), IR intensities (km/mol) in different normal modes; thermodynamic properties of  $\Delta G$ ,  $\Delta H$  in kcal/mol and  $\Delta S$  in cal/mol.K<sup>-1</sup> at 300K for ferulic acid.

Normal mode	IR Intensity	Frequency	$\Delta G \times 10^{-3}$	$\Delta H \times 10^{-3}$	$\Delta S$	Dipole moment
7	20.1093	67.2300				
9	48.3908	173.9136				
10	21.1470	256.0901				
19	13.3667	593.1856				
20	69.2086	630.6128				
22	13.4166	690.8565				
27	20.9287	1095.6171				
33	12.3962	1290.7644				
34	15.9229	1322.2006				
36	60.7994	1400.7510				
37	10.3508	1422.1133				
38	54.9214	1452.5102				
39	61.5063	1457.5534				
43	63.8002	1587.0391				
44	59.0184	1635.8803				
46	229.3311	1704.7879				
47	60.9898	1778.4595				
48	18.0560	1796.0738				
49	88.6499	1825.4359				
52	391.5317	1981.2124				
54	41.1629	2113.7971				
55	164.2962	2181.2207				
56	151.6760	2212.0669				
57	14.6167	3369.7689				
59	45.8486	3532.3312				
62	12.6548	3548.4760				
64	17.2721	3561.0077				
65	10.6338	4458.5282				
			-423.516	-423.487	94.974	3.8396

The polarization functions into the applied basis set in the computations always demonstrate a significant achievement on the simulation and modeling methods of theoretical levels. The normal modes of IR spectrum have been exploring the harmonic potential wells by analytic methods which keep the movement of all atoms at the same time in the vibration time scale leading to a natural definition of molecular vibrations (Table2).

The results of the above observations strongly suggest that ferulic acid in asafetida medicinal plant adsorbed on the surface of (6,6) armchair SWCNT at B3LYP/6-311+G(d,p) method in water solvent is predominantly due to basis set functions which are induced by a change in polarity of the environment which has approved that an increase in the dielectric constant increases the stability and efficiency of this drug for treating Omicron subvariants BA.4 and BA.5.

### 3.4. Frontier orbitals of HOMO & LUMO

The highest occupied molecular orbital energy (HOMO) and the lowest unoccupied molecular orbital energy (LUMO) have been calculated for ferulic acid (Table3). The HOMO, LUMO and band energy gap (ev) indicated the pictorial explanation of the frontier molecular orbital's and their respective positive and negative zones which are an important factor for identifying the molecular characteristics of ferulic acid in asafetida medicinal plant.

**Table3.** The HOMO (a.u.), LUMO (a.u.), band energy gap (ev) and other quantities (ev) for ferulic acid in asafetida drug.

Compound quantities*	(ev)
	$\mu$
$\chi$	0.1996
$\eta$	0.0274
$\zeta$	18.2481
$\psi$	0.7270

* $\mu = (E_{HOMO} + E_{LUMO})/2$ ;
$\chi = - (E_{HOMO} + E_{LUMO})/2$ ;
$\eta = (E_{LUMO} - E_{HOMO})/2$ ;
$\zeta = 1/(2\eta)$ ;
$\psi = \mu^2/(2\eta)$ .

Excited state	$E_{LUMO} \text{ (a.u.)} = -0.17216$
Ground state	$E_{HOMO} \text{ (a.u.)} = -0.22698$
$\Delta E = E_{LUMO} - E_{HOMO} \text{ (ev)}$	$= 1.4917$

In other words, the HOMO shows the capability for giving an electron while the LUMO as an electron acceptor exhibits the capability for achieving an electron. Therefore, the energy gap ( $\Delta E = E_{LUMO} - E_{HOMO}$ ) indicates the energy difference between frontier HOMO and LUMO orbital introducing the stability for the structure and unravels the chemical activity of the molecule. In this work, energy gap establishes how ferulic acid interacts with the surface of (6, 6) armchair CNT. Besides, frontier molecular orbitals run an important function in the optical and electrical properties like in UV-Vis spectra [50]. Moreover, for getting more conclusive approving in identifying the compound characteristics of this structure, a series of chemical reactivity parameters consisting of chemical potential ( $\mu$ ), electronegativity ( $\chi$ ), hardness ( $\eta$ ), softness ( $\zeta$ ), electrophilicity index ( $\psi$ ) has been done (Table3) [51-53].

The negative amounts of the chemical potential ( $\mu$ ) and the positive values of other quantities have exhibited a good stability of ferulic acid in asafetida drug through adsorption on the surface of (6,6) armchair CNT correlated with the trend of drug delivery (Table3). This stable complex and its binding pose within Omicron subvariants BA.4 and BA.5 viruses as an illustration of the molecular drug delivery.

### 3.5. Analysis of UV-VIS spectroscopy

There is a critical factor as an energy gap between HOMO and LUMO for recognizing the characteristics of molecular electrical transport [54-58]. Based on Frank-Condon principle, the maximum absorption peak (max) is related to an UV-visible spectrum to vertical excitation.

In this research, TD-DFT/6-311+G (d,p) calculations have been done to identify the low-lying excited states of ferulic acid in asafetida medicinal plant. The results contain the vertical excitation energies, oscillator strength and wavelength which have been presented in Figure4.



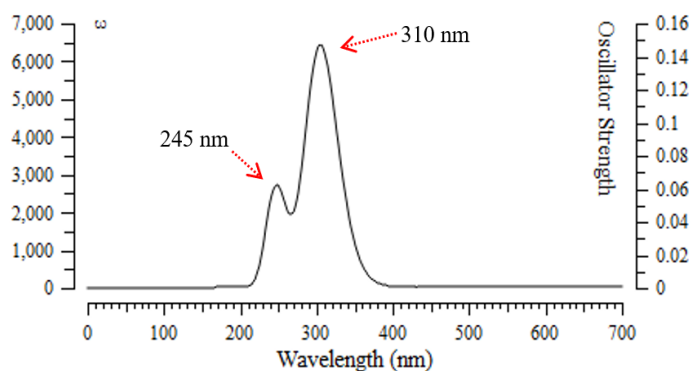


**Figure 4.** The graph of UV-VIS spectrum of ferulic acid in asafetida medicinal plant.

In the calculated value of UV-VIS spectrum for ferulic acid extracted from asafetida drug, there are two maximum adsorption bands between 200 nm-400 nm. The strong adsorptions have been observed in 245 nm and 310 nm, respectively (Figure4).

### CONCLUSION

Omicron subvariants BA.4 and BA.5 which are stimulating a new wave of infections in South Africa, might finally erupt in all over the world. BA.4 & BA.5 subvariants become developed from BA.2 and have identical sequences of SARS-CoV-2 spike (S) glycoprotein.

In this article, treating the Omicron subvariants BA.4 and BA.5 has been studied through asafetida medicinal plant due to ferulic acid extracted this natural drug. Ferulic acid has been calculated through adsorbing on the surface of (6, 6) armchair SWCNT at B3LYP/6-311+G (d,p) level of theory in water medium as the drug delivery method.

Asafetida has attracted much attention for the clinical treatment of Omicron subvariants BA.4 and BA.5 through adsorption of its effective compound of ferulic acid on the surface of (6,6) armchair SWCNT which introduces an efficient drug delivery system through charge distribution, NMR and IR spectroscopy on the optimized structure.

Moreover, the lowering of the energy gap ( $\Delta E = E_{\text{LUMO}} - E_{\text{HOMO}}$ ) has illustrated the charge transfer interactions taking place within ferulic acid. The atomic charges have donated the proper perception of the molecular theory and the energies of fundamental molecular orbitals.

### REFERENCES

- Hansen, J. et al. Studies in humanized mice and convalescent humans yield a SARS-CoV-2 antibody cocktail. *Science* **2020**, *369*, 1010-1014. doi:10.1126/science.abd0827.
- Shahriari, S.; Monajjemi, M.; Mollaamin, F., Determination of proteins specification with SARS- COVID-19 based ligand designing, *J. Chil. Chem. Soc.* **2022**, *67*, 5468-5476. doi: 10.4067/S0717-97072022000205468.
- Zost, S. J. et al. Potently neutralizing and protective human antibodies against SARS-CoV-2. *Nature* **2020**, *584*, 443-449, doi: 10.1038/s41586-020-2548-6.
- Mollaamin, F. Function of anti-cov structure using inh [1-6]-tyr160-met161-his162 complex. *Biointerface Res. Appl. Chem.* **2021**, *11*, 14433-14450. doi:10.33263/BRIAC116.1443314450.
- Jones, B. E. et al. The neutralizing antibody, LY-CoV555, protects against SARS-CoV-2 infection in nonhuman primates. *Sci Transl Med* **2021**, *13*, doi:10.1126/scitranslmed.abf1906.
- Mollaamin, F.; Esmkhani, R.; Monajjemi, M. Mutations in novel covid-19 make it more dangerous: Prevention via scientific approaches. *Biointerface Res. Appl. Chem.* **2021**, *11*, 10546-10558. doi: 10.33263/BRIAC113.1054610558.
- Shi, R. et al. A human neutralizing antibody targets the receptor-binding site of SARS-CoV-2. *Nature* **2020**, *584*, 120-124, doi:10.1038/s41586-020-2381-y.
- Monajjemi, M.; Shahriari, S.; Mollaamin, F. Evaluation of coronavirus families & COVID-19 proteins: Molecular modeling study. *Biointerface Res. Appl. Chem.* **2020**, *10*, 6039-6057. doi:10.33263/BRIAC105.60396057.

- Cao, Y. et al. BA.2.12.1, BA.4 and BA.5 escape antibodies elicited by Omicron infection. *bioRxiv*, **2022**, doi:10.1101/2022.04.30.489997.
- Mollaamin, F.; Monajjemi, M. Thermodynamic research on the inhibitors of coronavirus through drug delivery method. *J. Chil. Chem. Soc.* **2021**, *66*, 5195-5205. doi: 10.4067/S0717-97072021000205195.
- Khan, K. et al. Omicron sub-lineages BA.4/BA.5 escape BA.1 infection elicited neutralizing immunity. *medRxiv*, **2022**, doi:10.1101/2022.04.29.22274477.
- Zadeh, Mahsa Ali Akbari; Lari, Hadi; Kharghanian, Leyla; Balali, Ebrahim; Khadivi, Ramona; Yahyaei, Hooriye; Mollaamin, Fatemeh; Monajjemi, Majid, Density functional theory study and anti-cancer properties of shyshaq plant: In view point of nano biotechnology, *Journal of Computational and Theoretical Nanoscience*, **2015**, *12*, 4358-4367. https://doi.org/10.1166/jctn.2015.4366.
- Mollaamin, F. Physicochemical investigation of anti-COVID19 drugs using several medicinal plants, *J. Chil. Chem. Soc.*, **2022**, *67*(2), 5537-5546. doi: 10.4067/S0717-97072022000205537.
- Cannon, G.H.; Kaye, A.S. *The Persian Contributions to the English Language: An Historical Dictionary*. Otto Harrassowitz Verlag. **2001**, ISBN 978-3-447-04503-2.
- Khalili Hadad, B., Mollaamin, F., Monajjemi, M. Biophysical chemistry of macrocycles for drug delivery: A theoretical study, *Russian Chemical Bulletin*, **2011**, *60*, 238-241. doi:10.1007/s11172-011-0039-5.
- Li, J.; Zeng, M.; Shan, H.; Tong, C. Microneedle Patches as Drug and Vaccine Delivery Platform. *Current Medicinal Chemistry*. **2017**, *24*, 2413-2422. doi:10.2174/0929867324666170526124053.
- Tekade, R.K. *Basic fundamentals of drug delivery*. **2018**, ISBN 978-0-12-817910-9. OCLC 1078149382.
- Allen, T. M. Drug Delivery Systems: Entering the Mainstream. *Science*. **2004**, *303*, 1818-1822. doi:10.1126/science.1095833.
- Singh, A.P.; Biswas, A.; Shukla, A.; Maiti, P. Targeted therapy in chronic diseases using nanomaterial-based drug delivery vehicles. *Signal Transduct Target Ther.* **2019**, *4*, 33. doi:10.1038/s41392-019-0068-3.
- Cao, X.; Deng, W.; Fu, M. et al., Seventy-two-hour release formulation of the poorly soluble drug silybin based on porous silica nanoparticles: in vitro release kinetics and in vitro/in vivo correlations in beagle dogs. *European Journal of Pharmaceutical Sciences*, **2013**, *48*, 64-71. doi:10.1016/j.ejps.2012.10.012.
- Mollaamin, F.; Monajjemi, M. Harmonic Linear Combination and Normal Mode Analysis of Semiconductor Nanotubes Vibrations. *J. Comput. Theor. Nanosci* **2015**, *12*, 1030-1039. doi:10.1166/jctn.2015.3846.
- Zhang, L.; Xue, H.; Cao, Z.; Keefe, A.; Wang, J.; and Jiang, S. Multifunctional and degradable zwitterionic nanogels for targeted delivery, enhanced MR imaging, reduction-sensitive drug release, and renal clearance, *Biomaterials*, **2011**, *32*, 4604-4608. doi:10.1016/j.biomaterials.2011.02.064.
- Ghalandari, B.; Monajjemi, M.; Mollaamin, F. Theoretical Investigation of Carbon Nanotube Binding to DNA in View of Drug Delivery. *J. Comput. Theor. Nanosci* **2011**, *8*, 1212-1219. doi:10.1166/jctn.2011.1801.
- Monajjemi, M.; Honaparvar, B.; Khalili Hadad, B.; Ilkhani, A.; Mollaamin, F. Thermo-Chemical Investigation and NBO Analysis of Some anxiolytic as Nano- Drugs. *African journal of pharmacy and pharmacology* **2010**, *4*, 521-529.
- Khaleghian, M.; Zahmatkesh, M.; Mollaamin, F.; Monajjemi, M. Investigation of Solvent Effects on Armchair Single-Walled Carbon Nanotubes: A QM/MD Study. *Fuller. Nanotub. Carbon Nanostructures*, **2011**, *19*, 251-261. doi:10.1080/15363831003721757.
- Monajjemi, M. Liquid-phase exfoliation (LPE) of graphite towards graphene: An ab initio study. *Journal of Molecular Liquids* **2017**, *230*, 461-472. doi:10.1016/j.molliq.2017.01.044.
- Tahan, A.; Mollaamin, F.; Monajjemi, M. Thermochemistry and NBO analysis of peptide bond: Investigation of basis sets and binding energy. *Russian Journal of Physical Chemistry A* **2009**, *83*, 587-597. doi:10.1134/S003602440904013X.
- Monajjemi, M.; Baheri, H.; Mollaamin, F. A percolation model for carbon nanotube-polymer composites using the Mandelbrot-Given. *Journal of Structural Chemistry* **2011**, *52*, 54-59. doi: 10.1134/S0022476611010070.
- Mahdavian, L.; Monajjemi, M. Alcohol sensors based on SWNT as chemical sensors: Monte Carlo and Langevin dynamics simulation. *Microelectronics journal* **2010**, *41*, 142-149. doi: 10.1016/j.mejo.2010.01.011.
- Monajjemi, M. Cell membrane causes the lipid bilayers to behave as variable capacitors: A resonance with self-induction of helical proteins. *Biophysical Chemistry* **2015**, *207*, 114-127. doi:10.1016/j.bpc.2015.10.003.
- Frisch, M. J.; et al. Gaussian 16, Revision C.01, Gaussian, Inc., Wallingford CT, 2016.

32. a) Lee, C.; Yang, W.; Parr, R.G. Development of the Colle-Salvetti Correlation-Energy Formula into a Functional of the Electron Density. *Phys. Rev. B*, **1988**, *37*, 785-789. doi:10.1103/PhysRevB.37.785. (b) Stephens, P.J.; Devlin, F.J.; Chabalowski, C.F.; Frisch, M.J. Ab Initio Calculation of Vibrational Absorption and Circular Dichroism Spectra Using Density Functional Force Fields. *J. Phys. Chem.*, **1994**, *9*, 11623-11627. doi:10.1021/j100096a001.
33. Koch, W.; Holthausen, M.C. *A Chemist's Guide to Density Functional Theory*. 3-64, 93-104, 2nd edition, Wiley-VCH, Weinheim, Federal Republic of Germany, **2000**.
34. (a) Becke, A.D. Density-Functional Thermochemistry. III. The Role of Exact Exchange. *J. Chem. Phys.* **1993**, *98*, 5648-5652. doi:10.1063/1.464913. (b) Becke, A.D. Density-Functional Exchange-Energy Approximation with Correct Asymptotic Behavior. *Phys. Rev. A*. **1988**, *38*, 3098-3100. doi: 10.1103/PhysRevA.38.3098.
35. Bakhshi, K.; Mollaamin, F.; Monajjemi, M. Exchange and correlation effect of hydrogen chemisorption on nano V(100) surface: A DFT study by generalized gradient approximation (GGA). *J. Comput.Theor.Nanosci*, **2011**, *8*,763-768. doi: 10.1166/jctn.2011.1750.
36. Monajjemi, M.; Najafpour, J.; Mollaamin, F. (3,3)<sub>4</sub> Armchair carbon nanotube in connection with PNP and NPN junctions: Ab Initio and DFT-based studies. *Fullerenes Nanotubes and Carbon Nanostructures* **2013**, *21*, 213-232. doi:10.1080/1536383X.2011.597010.
37. Cramer, C.J.; Truhlar, D.G. PM3-SM3: A general parameterization for including aqueous solvation effects in the PM3 molecular orbital model. *J.Comp.Chem.* **1992**, *13*, 1089-1097. doi:10.1002/jcc.540130907.
38. Mollaamin, Fatemeh; Ilkhani, Alireza; Sakhaei, Neda; Bomsakhteh, Behnaz; Faridchehr, Afsaneh; Tohidi, Sogand; Monajjemi, Majid, Thermodynamic and solvent effect on dynamic structures of nano bilayer-cell membrane: Hydrogen bonding study, *Journal of Computational and Theoretical Nanoscience*, 2015, *12*, 3148-3154. doi:10.1166/jctn.2015.4092.
39. Mollaamin, F., Shahriari, S.; Monajjemi, M. Drug design of medicinal plants as a treatment of Omicron variant (COVID-19 VARIANT B.1.1.529) , *J. Chil. Chem. Soc.* **2022**, *67*, 5562-5570.
40. Giesen, D.J.; Gu, M.Z.; Cramer, C.J.; Truhlar, D.G. A Universal Organic Solvation Model. *J.Org.Chem.* **1996**, *61*, 8720-8721. doi:10.1021/jo9617427.
41. Onsager, L.J. Electric Moments of Molecules in Liquids. *J. Am. Chem. Soc.* **1936**, *58*, 1486-1493. doi: 10.1021/ja01299a050.
42. Tomasi, J. Cavity and reaction field: "robust" concepts. Perspective on Electric moments of molecules in liquids. *Theor.Chem.Acc.* **2000**, *103*, 196-199. doi: 10.1007/s002149900044.
43. Sarasia, E.M.; Afsharnezhad, S.; Honarparvar, B.; Mollaamin, F.; Monajjemi, M. Theoretical study of solvent effect on NMR shielding tensors of luciferin derivatives. *Phys Chem Liquids* **2011**, *49*, 561-571. doi: 10.1080/00319101003698992.
44. Mollaamin, F.; Monajjemi, M.; Salemi, S.; Baei, M.T. A Dielectric Effect on Normal Mode Analysis and Symmetry of BNNT Nanotube. *Fuller. Nanotub. Carbon Nanostructures* **2011**, *19*, 182-196. doi: 10.1080/15363831003782932.
45. Monajjemi, M.; Khaleghian, M.; Tadayonpour, N.; Mollaamin, F. The effect of different solvents and temperatures on stability of single-walled carbon nanotube: A QM/MD study. *Int. J. Nanosci.* **2010**, *09*, 517-529.
46. Monajjemi, M.; Baie, M.T.; Mollaamin, F. Interaction between threonine and cadmium cation in [Cd(Thr)] (n = 1-3) complexes: Density functional calculations , *Russian Chemical Bulletin* ,**2010**, *59*. 886-889, doi:10.1007/s11172-010-0181-5.
47. Monajjemi, M.; Robert, W.J.; Boggs, J.E. NMR contour maps as a new parameter of carboxyl's OH groups in amino acids recognition: A reason of tRNA-amino acid conjugation. *Chemical Physics* **2014**, *433*, 1-11. doi: 10.1016/j.chemphys.2014.01.017.
48. Fry, R.A.; Kwon, K.D.; Komarneni, S.; Kubicki, J.D.; Mueller, K.T. Solid-State NMR and Computational Chemistry Study of Mononucleotides Adsorbed to Alumina, *Langmuir*, **2006**, *22*, 9281-9286. doi: 10.1021/la061561s.
49. Monajjemi, M.; Mahdavian, L.; Mollaamin, F.; Khaleghian, M. Interaction of Na, Mg, Al, Si with carbon nanotube (CNT): NMR and IR study. *Russ. J. Inorg. Chem* **2009**, *54*, 1465-1473. doi: 10.1134/S0036023609090216.
50. Aihara, J.; Reduced HOMO-LUMO Gap as an Index of Kinetic Stability for Polycyclic Aromatic Hydrocarbons. *J. Phys. Chem. A* **1999**, *103*, 37, 7487-7495. doi: 10.1021/jp990092i.
51. Kohn, W.; Becke, A.D.; Parr, R.G. Density Functional Theory of Electronic Structure. *J. Phys. Chem.* **1996**, *100*, 12974-12980. doi: 10.1021/jp960669l. Parr, R.G. and Pearson, R.G. (1983) Absolute Hardness: Companion Parameter to Absolute Electronegativity. *J. Am. Chem. Soc.* **1983**, *105*, 7512-7516. doi: 10.1021/ja00364a005.
52. Politzer, P.; Abu-Awwad, F. A comparative analysis of Hartree-Fock and Kohn-Sham orbital energies. *Theor. Chem. Acc.* **1998**, *99*, 83-87. doi: 10.1007/s002140050307.
53. Silverstein, R.M.; Bassler, G.C.; Morrill, T.C. *Spectrometric Identification of Organic Compounds*, 5th ed., John Wiley & Sons, Inc., New York, **1981**.
54. Mollaamin, F.; Monajjemi, M. Application of DFT/TD-DFT Frameworks in the Drug Delivery Mechanism: Investigation of Chelated Bisphosphonate with Transition Metal Cations in Bone Treatment. *Chemistry* **2023**, *5*(1), 365-380. doi:10.3390/chemistry5010027.
55. Fatemeh Mollaamin & Majid Monajjemi, Molecular modelling framework of metal-organic clusters for conserving surfaces: Langmuir sorption through the TD-DFT/ONIOM approach. *MOLECULAR SIMULATION*, **2023**, *49* (4), 365-376. doi:10.1080/08927022.2022.2159996.
56. Mollaamin, F., Zare, K., Shahriari, S., Delivery of some Trapped Metal Elements in the Boron Nitride Nanocone: Application of Bio-Sensors in Cell Membrane using a DFT Evaluation, *Biointerface Research in Applied Chemistry*, **2023**, *13*(6), 1-19. doi: 10.33263/BRIAC134.345.
57. Sara Shahriari, Karim Zare, Fatemeh Mollaamin, Outlook of Covid-19 Curing through Structural and Electronic Properties of Natural Drugs, *Biointerface Research in Applied Chemistry*, **2023**, *13*(4), 1-15. doi:10.33263/BRIAC134.345.
58. Mollaamin, F., Monajjemi, M., Naeimi, M., Zare, K., Outlook of Covid-19 Curing through Structural and Electronic Properties of Natural Drugs, *Biointerface Research in Applied Chemistry*, **2023**, *13*(4), 1-21. doi: 10.33263/BRIAC134.396.